Experimental and Theoretical Study of the Formation of Silicon−Carbon Ion Species in Gaseous Silane/Ethene Mixtures

Paola Antoniotti, Carlo Canepa,* Lorenza Operti,* Roberto Rabezzana, Glauco Tonachini, and Gian Angelo Vaglio

Dipartimento di Chimica Generale ed Organica Applicata, Università di Torino, Corso Massimo d'Azeglio 48, 10125 Torino, Italy

Received: August 2, 1999; In Final Form: October 14, 1999

Results of gas-phase experiments and theoretical investigations are reported for ionic reactions in silane/ethene systems with the main interest in the formation and growth of species containing both silicon and carbon atoms. Ion/molecule reactions in different SiH_4/C_2H_4 mixtures have been studied with an ion trap mass spectrometer, determining variation of ion abundances with reaction time, reaction paths starting from primary ions of both reagents and reaction rate constants of the main processes. The best yield in formation of new Si−C bonds occurs in mixtures with an excess of silane, through processes of silicon-containing ions with ethene molecules. Since reactions of SiH_2^+ with ethene have been observed to play a major role in this system, they have been investigated by high-level ab initio methods. Structures and energies of intermediates ($SiC_2H_6^{\bullet+}$) and products ($SiC_2H_5^+$, $SiC_2H_4^{\bullet+}$, $SiCH_3^+$), as well as energy profiles of the pathways observed experimentally, have been determined. The initial step is formation of a $SiC_2H_6^{\bullet+}$ adduct at −44 kcal mol^{-1} with respect to the reactants, followed by isomerization reactions to four different structures through viable paths. Hydrogen atom loss to give $SiC_2H_5^+$ occurs through homolytic cleavage of a Si−H or C−H bond without energy barriers for the inverse process. Four different structures have been computed for $SiC_2H_4^{\bullet+}$ ion species, but only three of them are attainable by H_2 elimination from $SiC_2H_6^{\bullet+}$ or by isomerization. Formation of $SiCH_3^+$ involves three isomerization steps of the $SiC_2H_6^{\bullet+}$ adduct before the cleavage of a Si−C bond. Enthalpies of formation of all the structures have also been computed, and a good agreement with previously reported experimental data is generally observed for the most stable isomers.

Introduction

Over the past years, the study of the gas-phase ion chemistry of organosilicon compounds has experienced a rapid growth. The relevance of this research is related to the importance of these systems in the planetary chemistry and the reactivity of molecules present in interstellar clouds under the effect of ionizing radiations, cosmic rays, and low-wavelength photons.[1,2] Moreover, considerable interest is also due to the behavior of plasma and, in particular, to the preparation of amorphous silicon carbides, showing remarkable semiconducting properties, by chemical deposition of variously activated gaseous mixtures.[3−7] In the initial steps, ion species are involved mainly in chain propagation and the formation of precursors of the solid phase. The nature and abundance of the ion species give some indication of the optimal experimental conditions for the formation of amorphous solids of the desired composition and properties.

On the other hand, studies on gas-phase ion chemistry are strongly and continuously developing for the interest in the reactivity, reaction mechanisms, and kinetics of isolated ion species from a fundamental point of view.[8,9] In fact, information obtained by mass spectrometric methods on the intrinsic behavior of selected ions, in the absence of perturbations due to solvent or counterions,[3,4,10−15] is particularly useful for this research field. The experimental results can be directly correlated to the theoretical analysis of the processes under examination, which gives the relative stability of the structures of ion species, energetic profiles of reactions, and thermochemical data.[16−18]

Remarkable studies on mechanisms and kinetics of ion/molecule self-condensation reactions of SiH_4 and ab initio quantum chemical calculations on reaction pathways of the same system have been published recently.[3,16] Moreover, the gas-phase behavior in SiH_4/NH_3 and SiH_4/PH_3 mixtures has been studied in order to identify the best experimental conditions leading to silicon nitrides[11,19] or for direct phosphorus doping in the deposition of amorphous silicon films by radiolytic activation of appropriate gaseous systems.[15] Previously, the ionic gas-phase reactivity of SiH_4 with C_2H_4 and with C_2H_2 has been studied under high-pressure conditions[20,21] and ion/molecule reactions of Si^+ with a number of hydrocarbons, including ethane, ethene, and ethyne, have been investigated in detail.[22−24]

In our laboratory, the reaction mechanisms and the corresponding rate constants have been experimentally determined for the first nucleation steps leading to Si−C containing ions in silane/propane and silane/propene mixtures.[25]

In this paper, we report on the ionic overall reactivity, reaction mechanisms, and kinetics of silane/ethene systems in the gas phase, studied by ion trap mass spectrometry. The aim is to investigate the best conditions to form new silicon−carbon bonds for the deposition of amorphous silicon carbides from activated gaseous mixtures. On the basis of the experimental results, SiH_2^+ seems to be the most efficient precursor ion of the condensation process, eventually yielding the solid silicon carbide polymer. Therefore, its first nucleation step with ethene has been more deeply investigated by ab initio methods in order to determine structures, reaction energy profiles, and formation

10.1021/jp992722m CCC: $18.00
Published on Web 12/01/1999

enthalpies of the possible reaction intermediates and products. In fact, even if extensive theoretical research has been conducted on organosilicon species,[24,26−28] a large thermochemical database on ionic organosilicons, which could be very useful to assess a priori the feasibility of a process, is still lacking.

Experimental Section

Materials. Silane and ethene were commercially supplied by SIAD SpA with a stated purity of 99.99%. Prior to use, each of them was introduced into a flask containing anhydrous sodium sulfate in order to remove possible traces of water. Gas mixtures were prepared in the trap connecting the flasks to the gas inlet system of the instrument. Helium buffer gas was a research product from SIAD SpA at an extra-high degree of purity (99.9999%) and was used without further purification.

Mass Spectrometric Experiments. The methodology of ion trap mass spectrometry has been described elsewhere.[4,19] All experiments were performed on a Finnigan ITMS mass spectrometer. The instrument was maintained at 333 K in order to avoid thermal decomposition of silane and to obtain results comparable with similar systems studied previously.[25,26] The manifold and lines of the mass spectrometer were frequently baked-out to prevent side reactions with water background. Samples were admitted to the trap through a modified inlet system, which permits the simultaneous introduction of three gases through different lines and the use of a leak or a pulsed valve. The pressures were measured by a Bayard Alpert ionization gauge and were typically in the range 2.0×10^{-7} to 1.0×10^{-6} Torr for silane and ethene, while helium was added to a total pressure of about 5.0×10^{-4} Torr. The pulsed gas profile was approximately 1.5 s wide and reached a maximum after about 250 ms; its pressure was previously set at 1.0×10^{-6} Torr behind the valve. The indicated pressures of the reagent gases were corrected on the basis of two factors: calibration of the gauge[4] and relative sensitivity of the gauge to different gases (1.70 for SiH_4, 1.87 for C_2H_4).[29] The scan modes used to study the overall behavior of different silane/ethene mixtures (no selective isolation of ions, reaction times up to 1 s) or to determine reaction mechanisms (selective isolation of ions, reaction times up to 500 ms) and rate constants (selective isolation of ions, reaction times up to 50 ms) have been already described in detail, together with the calculation procedures.[14,15,17,19] In kinetic experiments, isolation of the reacting ion species is alternatively achieved by the apex method or by resonance ejection, the latter giving a lower content of excitation energy on the selected ions. Similarity of results indicates that collisional cooling is effective in removing most of the internal energy, as it is also evidenced by the single-exponential decay of the abundances of the reacting species. In all experiments, ionization was obtained by bombardment with an electron beam at 35 eV average energy for times in the range 1−10 ms, ions were reacted keeping $m/z = 10$ as the start mass ($q_z = 0.908$) and were detected in the 10−300 u mass range.

Methods of Calculation. Theoretical calculations were carried out utilizing gradient geometry optimization procedures[30] implemented in the Gaussian94 system of programs.[31] All structures were fully optimized at the DFT level with the three-parameters hybrid functional of Becke,[32a] together with the correlation functional of Lee, Yang, and Parr[32b] (B3LYP)[32c] in conjunction with the 6-311G(d,p) basis set.[32d] This theory level will be indicated as DFT(B3LYP)/6-311G(d,p) in the following. Vibrational frequency calculations were used to characterize all stationary points as either minima or first-order saddle points. The Complete Basis Set method of Petersson[33] (CBS-Q) and the G2 method of Pople[34] have been used to compute thermochemical data. Thermochemical data have been computed using unscaled frequencies in the harmonic oscillator rigid rotor approximation.[35] All open shell species show little spin contamination and the reported energies are unprojected, as suggested by Wittbrodt and Schlegel.[36]

Results and Discussion

Mass Spectrometric Determinations. Three different kinds of experiments were performed with the specific purposes of (a) studying the formation and growth of silicon- and carbon-containing ion species (mixed ions) in mixtures with different partial pressure ratios of silane and ethene at about 1.2×10^{-6} Torr total pressure (no isolation of ions, reaction time up to 1 s), (b) determining the reaction mechanisms of the most important ions with a particular attention to those pathways leading to the formation of ions with a high number of silicon and carbon atoms (isolation of selected ions, reaction time up to 500 ms), and (c) measuring the reaction rate constants of the most significant processes observed in the previous experiments (isolation of selected ions, reaction time up to 50 ms by 0.2 ms steps).

Three different mixtures at constant total pressure were considered, which consist of silane and ethene in the approximate ratios 1:5 [$p(SiH_4) = 2.1 \times 10^{-7}$ Torr, $p(C_2H_4) = 9.8 \times 10^{-7}$ Torr], 1:1 [$p(SiH_4) = 6.2 \times 10^{-7}$ Torr, $p(C_2H_4) = 6.5 \times 10^{-7}$ Torr], and 5:1 [$p(SiH_4) = 1.0 \times 10^{-6}$ Torr, $p(C_2H_4) = 1.8 \times 10^{-7}$ Torr]. Ionization of the two reacting molecules produces the SiH_n^+ ($n = 0-3$) and $C_2H_n^+$ ($n = 2-4$) ion families which are trapped in the cell of the mass spectrometer and react with both neutral for increasing reaction times up to 1 s. During this time, many ion/molecule reactions occur yielding, among others, ions containing silicon and carbon bonded together. In 1 s, several ion families are formed in successive reactions and products are detected, which are formed after four reaction steps, even if in very low abundance. Considering all the possible mixed ions produced starting from primary ions of silane (Scheme 1), only the following were

SCHEME 1

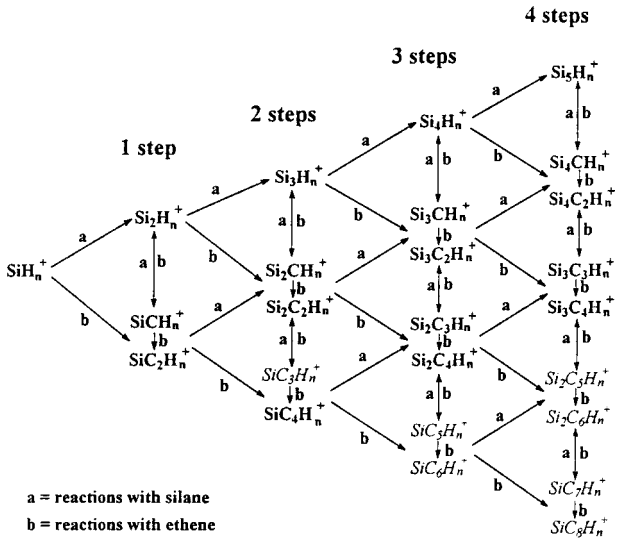

experimentally observed: $SiCH_n^+$ ($n = 3, 5$); $SiC_2H_n^+$ ($n = 4-7$); $Si_2CH_n^+$ ($n = 5, 6$); $Si_2C_2H_n^+$ ($n = 4-7$); $SiC_4H_n^+$ ($n = 6, 7$); $Si_3CH_n^+$; $Si_3C_2H_n^+$; $Si_2C_3H_n^+$; $Si_2C_4H_n^+$; $Si_4CH_n^+$; $Si_4C_2H_n^+$; $Si_3C_3H_n^+$; $Si_3C_4H_n^+$, which are shown in the scheme in bold characters. In this kind of experiment, without isolation

of ions, it is not possible to univocally identify species formed in three or four reaction steps giving a precise number of hydrogen atoms, as the most abundant isotope of silicon (^{28}Si) has the same nominal mass as the C_2H_4 moiety and an overlap of ion clusters may occur. As an example, ions such as $SiC_6H_n^+$ can partially overlap the $Si_2C_4H_n^+$ ion family, depending on the value of n and their common precursors, $SiC_4H_n^+$ ($n = 6$, 7), show rather high abundances in all mixtures examined. However, the formation of $SiC_6H_n^+$ species can be neglected as the abundances of ions at m/z from 109 to 115 are negligible up to 1 s of reaction in the mixture containing an excess of ethene and show the maximum yield in the presence of silane in excess.

Variation of the abundances of the observed ion families, together with the products of three ($Si_3CH_n^+$, $Si_3C_2H_n^+$, $Si_2C_3H_n^+$, $Si_2C_4H_n^+$) and four ($Si_4CH_n^+$, $Si_4C_2H_n^+$, $Si_3C_3H_n^+$, $Si_3C_4H_n^+$) reaction steps grouped together, are reported in parts a−c of Figure 1 for the three silane/ethene mixtures. The $SiCH_n^+$ ($n = 3$, 5) ions are by far the most abundant in the 1:5 and 1:1 systems, reaching the maximum value of almost 30% in the 1:1 mixture. It is worth noting that the abundances of the other ions never exceed 6% in the SiH_4/C_2H_4 1:5 mixture. Also, in the 1:1 system, only the $SiC_2H_n^+$ ($n = 4-7$) ion species display an appreciable abundance, whereas the remaining families are lower than 5% at any time here considered. In contrast, in the silane/ethene 5:1 mixture, $SiCH_n^+$ and $SiC_2H_n^+$ ions show a very similar trend. Moreover, in the same system, ions formed in successive reaction steps, such as $Si_2C_2H_n^+$ ($n = 4-7$) or the three reactions products, display the highest abundances of the mixtures examined after 1 s of reaction.

A second set of experiments has been performed with isolation and storage of selected ions. The $SiCH_n^+$ ($n = 3$, 5) ions are very abundant as they are formed in several ion/molecule processes and react further only at very long reaction time. Therefore, they do not contribute to the growth of the mixed ions containing both carbon and silicon. In the same way, it has been determined that $Si_2C_2H_n^+$ ($n = 4-7$) ion species are very important in the chain propagation as they react with rather high rate constants with both silane and ethene yielding the $Si_3CH_n^+$, $Si_3C_2H_n^+$, $Si_2C_3H_n^+$, and $Si_2C_4H_n^+$ ion families. Moreover, the $Si_2C_2H_n^+$ ($n = 4-7$) ions are given in part by the $SiC_2H_n^+$ ($n = 4-7$) species reacting with silane. This behavior can be deduced from Scheme 2, which shows as an example the mechanism of the processes involved in the formation of mixed ions starting from SiH_2^+ primary ions. The remaining SiH_n^+ ($n = 0$, 1, 3) ions of silane react in similar paths, the main difference being the lower number of products observed with respect to SiH_2^+. It follows that the growth of the mixed ions seems to proceed mainly through the following favored sequence:

SCHEME 2

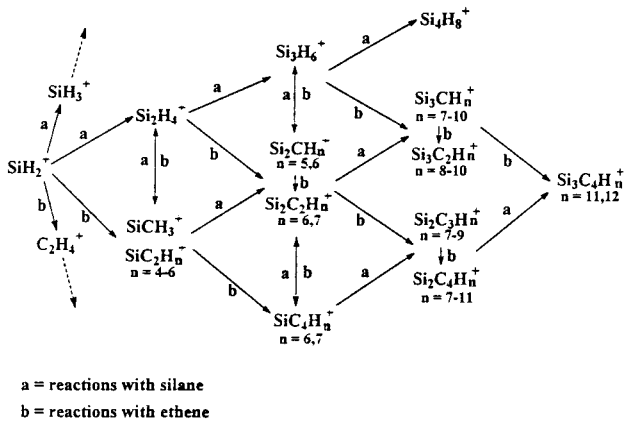

$$SiC_2H_n^+ \text{ (1 step)} \rightarrow Si_2C_2H_n^+ \text{ (2 steps)} \rightarrow Si_2C_3H_n^+, Si_2C_4H_n^+, Si_3CH_n^+, Si_3C_2H_n^+ \text{ (3 steps)} \quad (1)$$

This hypothesis is in agreement with the variation of abundances shown in Figure 1, where the experimental conditions, leading to the highest abundance of $SiC_2H_n^+$ ($n = 4-7$) species, i.e., SiH_4/C_2H_4 5:1, also give the best yield for both $Si_2C_2H_n^+$ ($n = 4-7$) ions and the products of three reaction steps. This trend is further confirmed by data displayed in Figure 2, which reports the variation of the sum of ion abundances of all mixed ions save $SiCH_n^+$ ($n = 3$, 5), as a function of reaction time for the three silane/ethene mixtures. The highest yield is given by the SiH_4/C_2H_4 5:1 mixture, which is almost twice that in the 1:5 mixture. However, it is worth noting that the behavior of the 1:1 silane/ethene system is rather similar to that of the 5:1 one. Such trend can be due to the involvement of ethene as a neutral reagent in the paths described in Schemes 1 and 2 and of its primary ions ($C_2H_n^+$, $n = 2-4$) together with $C_2H_5^+$ as starting species of the same sequence, as they form SiH_n^+ ($n = 2$, 3) and $SiC_2H_n^+$ ($n = 3-7$) ions in reactions with silane (Scheme 3). Therefore, experimental results indicate that the presence

SCHEME 3

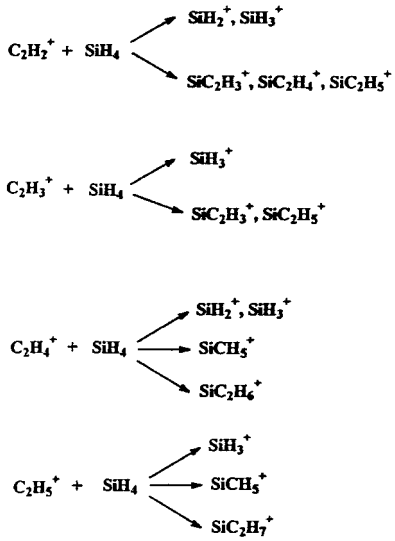

of an excess of ethene in the SiH_4/C_2H_4 mixtures strongly prevents the formation and growth of mixed ions, favoring self-condensation processes. Such behavior is consistent with simple considerations based on the energies of bonds between the atoms involved in these systems. In fact, according to the literature,[37] bond energies decrease in the order C−C (145 ± 5 kcal mol^{-1}), C−Si (107.9 kcal mol^{-1}), Si−Si (78.1 ± 2.4 kcal mol^{-1}). It follows that formation of new bonds with carbon (ethene) is the most favored path for primary ions of both ethene and silane, yielding mixed species only in the latter case.

However, as kinetic factors are also likely to play an important role in these systems, the rate constants for the most significant processes occurring in silane/ethene mixtures have been experimentally determined and are shown in Tables 1 and 2. Collisional rate constants calculated according to the Langevin theory,[38] and reaction efficiencies are also reported in these tables. Each experimental value is the mean of at least three different runs performed on different days using the silane/ethene

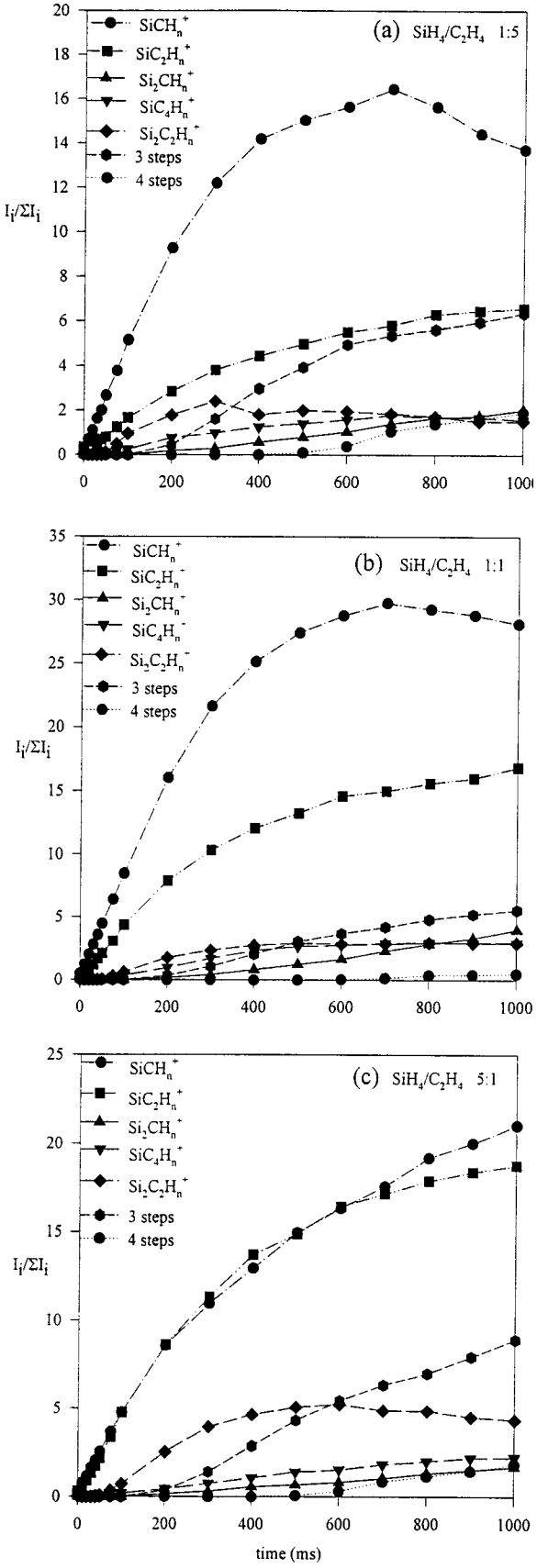

Figure 1. Variation of the abundances with reaction time of the $SiCH_n^+$, $SiC_2H_n^+$, $Si_2CH_n^+$, $SiC_4H_n^+$, and $Si_2C_2H_n^+$ ion families and of ions produced in three or four reaction steps for silane/ethene mixtures in the approximate ratios 1:5 (a), 1:1 (b), and 5:1 (c).

1:1 mixture in the conditions described above. Rate constants lower than 1×10^{-11} cm^3 molecule^{-1} s^{-1} could not be measured

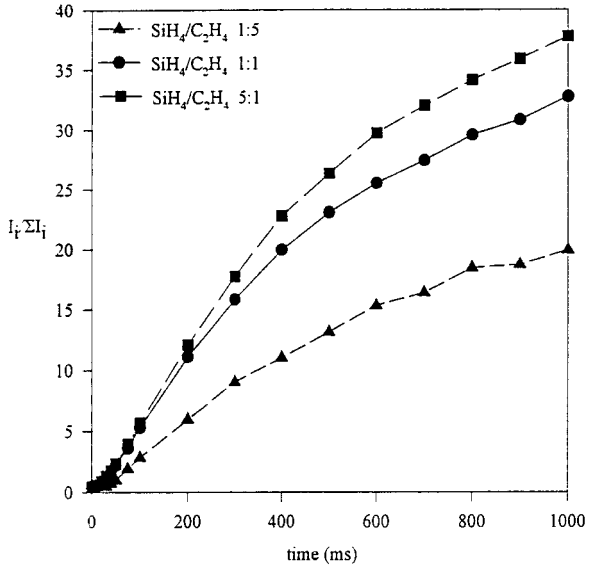

Figure 2. Variation of the sum of the abundances of mixed ions, excluding $SiCH_n^+$, as a function of reaction time for each of the 1:5, 1:1, and 5:1 silane/ethene mixtures.

with a good reliability and are not displayed in these tables. As the main interest of this paper is the study of the conditions leading to the formation of silicon−carbon bonds, Table 1 reports reactions of ions containing carbon and hydrogen with silane and of ions containing silicon and hydrogen with ethene, whereas rate constants of self-condensation processes are not shown. However, they have been determined and compared with already published results[4,41] and show a general good agreement. In Table 2, the rate constants of reactions of mixed ions with both neutral reagents are reported for those species having an abundance sufficiently high to give reproducible results. Rate constants of reactions of the isobaric ions at *m*/*z* 28 (Si^+ and $C_2H_4^+$) and 29 (SiH^+ and $C_2H_5^+$) could not be determined as the use of a pulse valve does not permit any control of the pressure of the pulsed gas and, therefore, a direct comparison of their reactivity with that of SiH_2^+ and SiH_3^+ is not possible. However, isolating the silane primary ions, SiH_n^+ ($n = 0-3$), and pulsing ethene in the trap in the same experimental conditions, it was possible to determine that SiH_2^+ is the most reactive leading to the highest number of product ions displaying high abundances. Moreover, a comparison can be drawn on the reaction rate constants of secondary ($Si_2H_n^+$) and tertiary ($Si_3H_n^+$) silane ions reported in Table 1, which indicates that the most reactive species within each family, $Si_2H_4^+$ and $Si_3H_6^+$, respectively, originate from SiH_2^+. A similar trend is also observed in Table 2, where mixed ions such as $SiC_2H_4^+$, given by SiH_2^+, react with both silane and ethene with rather good efficiency and the same occurs for their products $Si_2C_2H_n^+$ ($n = 6, 7$). Finally, a comparison of our results on reactions of SiH_n^+ ($n = 2, 3$) ions and ethene, with those obtained by Lampe and co-workers,[20,21] shows a good agreement as far as reaction products and overall rate constants are concerned, whereas products distributions slightly differ for SiH_2^+.

According to the experimental results described above, which indicate SiH_2^+ as the most important primary ion involved in the formation of species containing silicon and carbon atoms together, theoretical calculations have been performed on the structures and energetics of mixed products of the first step of the reaction of SiH_2^+ with C_2H_4.

Theoretical Study. The theoretical study has been aimed to point out the possible pathways that lead from the SiH_2^+ and

TABLE 1: Rate Constants for Reactions of $C_nH_m^+$ Ions with Silane and of $Si_nH_m^+$ Ions with Ethene in Silane/Ethene Mixtures[a]

reactants	product ions and rate constants (k_{exp})	$\sum k_{exp}$	$k_{collisional}$[b]	efficiency[c]
$C_2H_2^+ + SiH_4$	SiH_2^+ (2.4), SiH_3^+ (2.2), $SiC_2H_4^+$ (0.87), $SiC_2H_5^+$ (3.4)	8.9	12.85	0.69
$C_2H_3^+ + SiH_4$	SiH_3^+ (6.6), $SiC_2H_3^+$ (0.67)	7.3	12.72	0.57
$C_3H_3^+ + SiH_4$	$SiCH_3^+$ (0.16), $SiCH_5^+$ (0.40)	0.56	11.61	0.048
$C_3H_5^+ + SiH_4$	$SiCH_5^+$ (6.7), $SiC_2H_3^+$ (0.40)	7.1	11.48	0.62
$SiH_2^+ + C_2H_4$	$C_2H_4^+$ (1.4), $SiCH_3^+$ (6.4), $SiC_2H_4^+$ (1.4), $SiC_2H_5^+$ (0.65)	9.8	12.66	0.77
$SiH_3^+ + C_2H_4$	$SiCH_3^+$ (1.3), $SiCH_5^+$ (4.4), $SiC_2H_5^+$ (0.60), $SiC_2H_7^+$ (1.0)	7.3	12.56	0.58
$Si_2H_2^+ + C_2H_4$	$Si_2CH_4^+$ (0.95), $Si_2C_2H_4^+$ (0.89), $Si_2C_2H_5^+$ (1.2)	3.0	11.09	0.27
$Si_2H_3^+ + C_2H_4$	$Si_2CH_5^+$ (1.8), $Si_2C_2H_5^+$ (0.70)	2.5	11.06	0.23
$Si_2H_4^+ + C_2H_4$	$Si_2CH_6^+$ (0.49), $Si_2C_2H_6^+$ (3.8)	4.3	11.03	0.39
$Si_2H_5^+ + C_2H_4$	$Si_2CH_7^+$ (0.71), $Si_2C_2H_7^+$ (0.71)	1.42	11.00	0.13
$Si_3H_5^+ + C_2H_4$	$Si_2C_2H_5^+$ (0.69), $Si_3C_2H_7^+$ (4.3), $Si_3C_2H_9^+$ (0.11)	5.1	10.44	0.49
$Si_3H_6^+ + C_2H_4$	$Si_2C_2H_6^+$ (0.92), $Si_3CH_{10}^+$ (1.1), $Si_3C_2H_8^+$ (3.9)	5.9	10.43	0.56
$Si_3H_7^+ + C_2H_4$	$Si_2C_2H_7^+$ (0.19), $Si_3CH_{11}^+$ (0.66), $Si_3C_2H_9^+$ (1.0)	1.8	10.42	0.17

[a] Rate constants are expressed as 10^{-10} cm^3 molecule^{-1} s^{-1}; uncertainty is within 20%. [b] Collisional rate constants have been calculated according to the Langevin theory taking polarizability of silane (4.339×10^{-24} cm^3) from ref 39 and that of ethene (4.252×10^{-24} cm^3) from ref 40. [c] Efficiency has been calculated as the ratio $k_{exp}/k_{collisional}$.

TABLE 2: Rate Constants for Reactions of $Si_nC_mH_x^+$ Ions with Silane and Ethene in Silane/Ethene Mixtures[a]

reactants	product ions and rate constants (k_{exp})	$\sum k_{exp}$	$k_{collisional}$[b]	efficiency[c]
$SiC_2H_4^+ + C_2H_4$	$SiC_4H_6^+$ (0.78), $SiC_4H_7^+$ (3.5)	4.3	11.16	0.38
$+ SiH_4$	$Si_2H_4^+$ (2.0), $Si_2C_2H_6^+$ (1.5)	3.5	10.78	0.32
$SiC_2H_5^+ + C_2H_4$	$SiC_4H_7^+$ (1.2)	1.2	11.12	0.11
$+ SiH_4$	$Si_2H_3^+$ (1.5), $Si_2C_2H_7^+$ (0.46)	2.0	10.75	0.19
$SiC_4H_7^+ + SiH_4$	$Si_2C_3H_7^+$ (0.33), $Si_2C_4H_7^+$ (0.54)	0.87	10.13	0.086
$Si_2C_2H_4^+ + C_2H_4$	$Si_2C_4H_6^+$ (0.29), $Si_2C_4H_8^+$ (1.0)	1.3	10.52	0.12
$+ SiH_4$	$Si_3C_2H_6^+$ (1.0)	1.0	10.11	0.099
$Si_2C_2H_5^+ + C_2H_4$	$Si_2H_3^+$ (0.55), $Si_2C_4H_7^+$ (0.38), $Si_2C_4H_9^+$ (0.75)	1.68	10.50	0.16
$+ SiH_4$	$Si_3C_2H_7^+$ (0.95)	0.95	10.09	0.094
$Si_2C_2H_6^+ + C_2H_4$	$Si_2C_3H_7^+$ (2.0), $Si_2C_4H_9^+$ (3.2)	5.2	10.49	0.50
$+ SiH_4$	$Si_3C_2H_8^+$ (1.8), $Si_3C_2H_{10}^+$ (0.72)	2.5	10.08	0.25
$Si_2C_2H_7^+ + C_2H_4$	$Si_2C_3H_8^+$ (0.19), $Si_2C_4H_9^+$ (0.35), $Si_2C_4H_{10}^+$ (0.41), $Si_2C_4H_{11}^+$ (1.9)	2.8	10.47	0.27
$+ SiH_4$	$Si_3CH_7^+$ (0.42)	0.42	10.06	0.042

[a] Rate constants are expressed as 10^{-10} cm^3 molecule^{-1} s^{-1}; uncertainty is within 20%. [b] Collisional rate constants have been calculated according to the Langevin theory taking polarizability of silane (4.339×10^{-24} cm^3) from ref 39 and that of ethene (4.252×10^{-24} cm^3) from ref 40. [c] Efficiency has been calculated as the ratio $k_{exp}/k_{collisional}$.

C_2H_4 reacting species, through the formation of the $SiC_2H_6^{\bullet+}$ (**1**) intermediate, to the hydrogen atom, hydrogen molecule, or methyl group dissociation to give $SiC_2H_5^+$ (**2**), $SiC_2H_4^{\bullet+}$ (**3**), and $SiCH_3^+$ (**4**) ions, respectively.

Since these processes involve a change in number of particles, we chose to discuss the energy profile in term of free energies at 298 K.

A. Formation and Isomerization of $SiC_2H_6^{\bullet+}$ Ions. The ion/molecule interaction between SiH_2^+ and C_2H_4 is highly exoergonic and the complexes **1a, 1b, 1c, 1d,** and **1e** have enough internal energy to overcome most of the subsequent barriers.

$$SiH_2^+ + C_2H_4 \rightarrow SiC_2H_6^{\bullet+}\ (\mathbf{1a}) \quad \Delta G = -43.6 \text{ kcal mol}^{-1} \tag{2}$$

The structures and energies of different isomers corresponding to the same formula have been optimized and are reported in Figure 3 together with the isomerization transition structures. The corresponding enthalpies and free energies calculated at DFT(B3LYP)/6-311G(d,p), CBS-Q and G2 levels of theory are shown in Table 3. The bridged structure **1a** is the first on the reaction coordinate. Its silicon atom interacts symmetrically with the two carbon atoms of ethene and the spin density is almost equally shared between the two interacting fragments. The C−C distance is elongated 0.100 Å with respect to ethene. The two isomer open intermediates **1b** and **1c** lie 7.3 and 17.7 kcal mol^{-1} above **1a**, respectively. As the hydrogen atoms are shifted from the silicon moiety to the hydrocarbon part of the structure, the spin density becomes more localized on the former. Structure **1c** has a full unpaired electron on the silicon cation, which is weakly interacting with ethane. Transition structures TS-**1a1b** and TS-**1b1c** represent subsequent hydrogen migrations from silicon to carbon connecting **1a** to **1b** and **1c** as shown in Figure 3. TS-**1b1c**, relevant to a 1,2 migration, is less stable than TS-**1a1b**, pertinent to a 1,3 migration, reflecting the difference in stability between minima **1b** and **1c**. Homolytic cleavage of the C−C bond in **1c** leads to the silene-like species **1d**, the most stable species both on the electronic and free energy surfaces, through TS-**1c1d**. The overall process

$$\mathbf{1a} \rightarrow \text{TS-}\mathbf{1a1b} \rightarrow \mathbf{1b} \rightarrow \text{TS-}\mathbf{1b1c} \rightarrow \mathbf{1c} \rightarrow \text{TS-}\mathbf{1c1d} \rightarrow \mathbf{1d} \tag{3}$$

is exoergonic by 16.5 kcal mol^{-1}, involving a barrier of only 3.2 kcal mol^{-1} (Figure 3).

The 1,2 hydrogen migration from C^2 to C^1 is a slower process since it involves TS-**1a1e**, 6.4 kcal mol^{-1} above the energy of the reactants. The spin density in TS-**1a1e** is mostly localized on the C^2 atom, whose distance from C^1 is significantly increased by 0.248 Å. Compound **1e** can also be formed from **1b** via 1,2 hydrogen migration. TS-**1b1e** at −14.2 kcal mol^{-1} is the transition structure for such migration.

B. H Dissociation from $SiC_2H_6^{\bullet+}$ and Isomerization of $SiC_2H_5^+$ Ions. Each of the ions $SiC_2H_6^{\bullet+}$ **1a, 1b, 1c, 1d,** and **1e** can homolytically eliminate a hydrogen atom leading to singlet cations **2a, 2b, 2c,** and **2d** (Figure 4). The enthalpies and free energies of the $SiC_2H_5^+$ products relative to isolated reactants are reported in Table 4. The differences in free energies of the

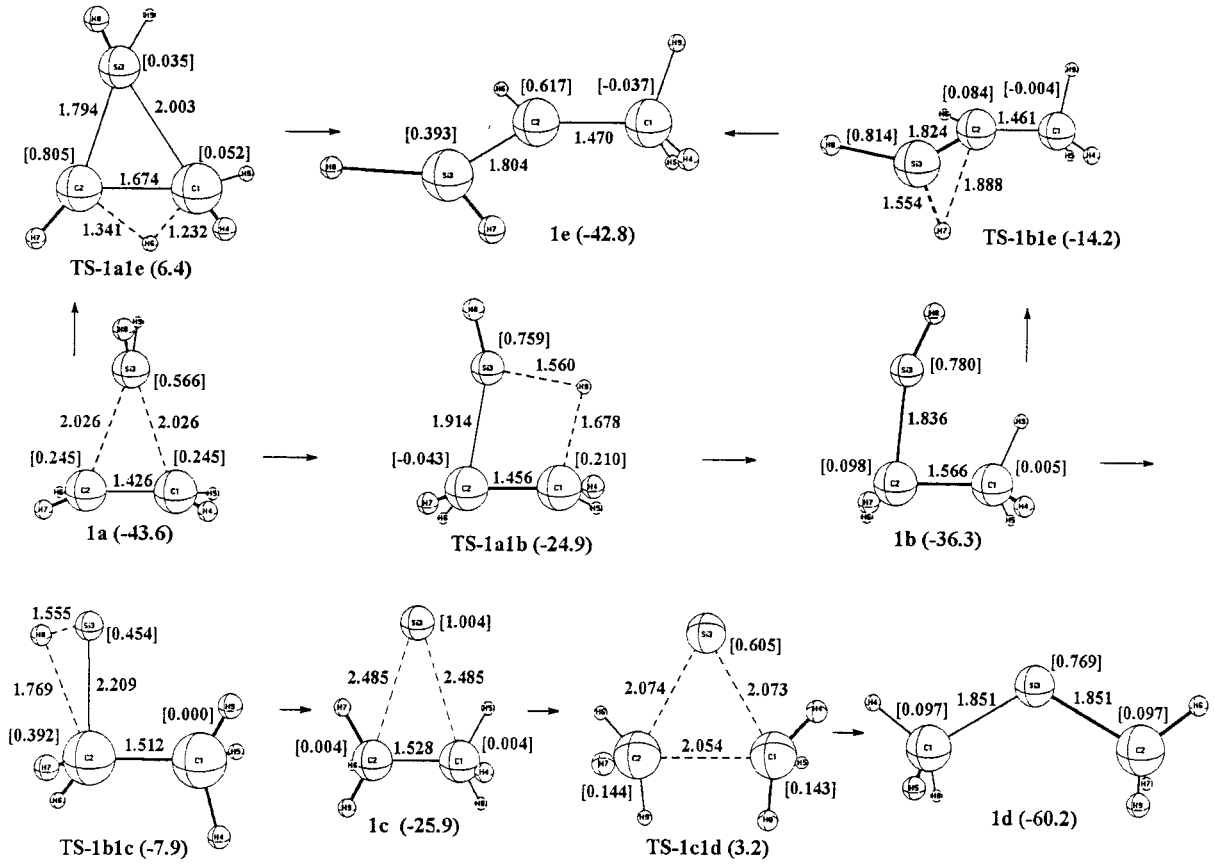

Figure 3. Intermediates and transition structures of the $SiC_2H_6^{\bullet+}$ system at the DFT(B3LYP)/6-311G(d,p) level of theory. Distances are in angstroms. Differences in free energy in kcal mol^{-1} with respect to isolated reactants $SiH_2^+ + C_2H_4$ are given in parentheses; total spin densities are given in brackets.

TABLE 3: Enthalpies and Free Energies (kcal mol^{-1}) at 298 K of the $SiC_2H_6^{\bullet+}$ System Relative to Reactants $SiH_2^+ + C_2H_4$ at Various Levels of Theory

	DFT(B3LYP)/6-311G(d,p)			CBS-Q		G2	
species	ΔH_{298}	ΔG_{298}	$\langle S^2\rangle$	ΔH_{298}	ΔG_{298}	ΔH_{298}	$\Delta \mathbf{G}_{298}$
1a	−54.5	−43.6	0.7524	−58.5	−47.0	−57.8	−46.3
1b	−47.2	−36.3	0.7521	−48.4	−38.6	−47.9	−38.2
1c	−36.3	−25.9	0.7539	−38.3	−29.0	−38.4	−29.2
1d	−68.3	−60.2	0.7517	−70.3	−62.1	−67.3	−59.1
1e	−53.2	−42.8	0.7526	−53.0	−42.7	−49.8	−39.6
TS-1a1b	−36.6	−24.9	0.7550				
TS-1b1c	−17.5	−7.9	0.7557				
TS-1c1d	−7.6	3.2	0.7532				
TS-1a1e	−4.8	6.4	0.7549				
TS-1b1e	−25.2	−14.2	0.7543				

following processes, formally leading from $SiC_2H_6^{\bullet+}$ to $SiC_2H_5^+$, are reported in parentheses in kcal mol^{-1}.

$$SiC_2H_6^{\bullet+} \rightarrow SiC_2H_5^+ (\mathbf{2}) + H \quad (4)$$

$$\mathbf{1a} \rightarrow \mathbf{2a} + H\ (42.3) \quad (5)$$

$$\mathbf{1a} \rightarrow \mathbf{2b} + H\ (78.7) \quad (6)$$

$$\mathbf{1b} \rightarrow \mathbf{2c} + H\ (39.1) \quad (7)$$

$$\mathbf{1b} \rightarrow \mathbf{2d} + H\ (49.4) \quad (8)$$

$$\mathbf{1c} \rightarrow \mathbf{2c} + H\ (28.7) \quad (9)$$

$$\mathbf{1e} \rightarrow \mathbf{2a} + H\ (41.6) \quad (10)$$

Since homolytical cleavages typically proceed without an electronic barrier for the inverse process, a search for transition structures connecting **1a**−**1e** to **2a**−**2d** was not attempted. Structures **2a** and **2c** are close in energy to the isolated reactants (−1.3 and 2.8 kcal mol^{-1}, respectively), while **2b** and **2d** lie well above (35.1 and 13.1 kcal mol^{-1}). **2a** and **2b** are allyl-type structures that differ greatly in their bonding. While **2a** is unsymmetrical with the SiH_2 group on one end and a full double bond between the two carbon atoms, **2b** is symmetric and does not exhibit a double bond. The most favorable path leading to **2a** thus involves homolytic cleavage of a C−H bond of **1a** or **1e**; that leading to **2c** involves cleavage of the Si−H bond of **1b**. The two structures **2c** and **2d** are also connected by a hydrogen migration transition structure (TS-**2c2d**), whose energy is in excess by 13.2 kcal mol^{-1} with respect to isolated reactants. Its geometry is very close to **2d**, and a further elongation of the C^1-H^8 distance by 0.246 Å leads to the product.

C. H_2 Dissociation from $SiC_2H_6^{\bullet+}$ and Isomerization of $SiC_2H_4^{\bullet+}$ Ions. Structures **3a, 3b, 3c,** and **3d**, already described by Ketvirtis et al.,[24] have been recomputed at the DFT(B3LYP)/6-311G(d,p) level and are shown in Figure 5. Table 5 reports the corresponding enthalpies and free energies of their formation reactions. They can formally derive either from any of the ions $SiC_2H_6^{\bullet+}$ by elimination of a hydrogen molecule

$$SiC_2H_6^{\bullet+} \rightarrow SiC_2H_4^{\bullet+} (\mathbf{3}) + H_2 \quad (11)$$

or, from $SiC_2H_5^+$, by homolytic cleavage of a C−H or Si−H bond:

$$SiC_2H_5^+ \rightarrow SiC_2H_4^{\bullet+} (\mathbf{3}) + H \quad (12)$$

However, process 12 would require breaking a Si−H or C−H bond in structures **2a**−**2d**, leading to the high-energy products $SiC_2H_4^{\bullet+}$ (**3**) + 2H$^{\bullet}$. In process 11, the two hydrogen atoms

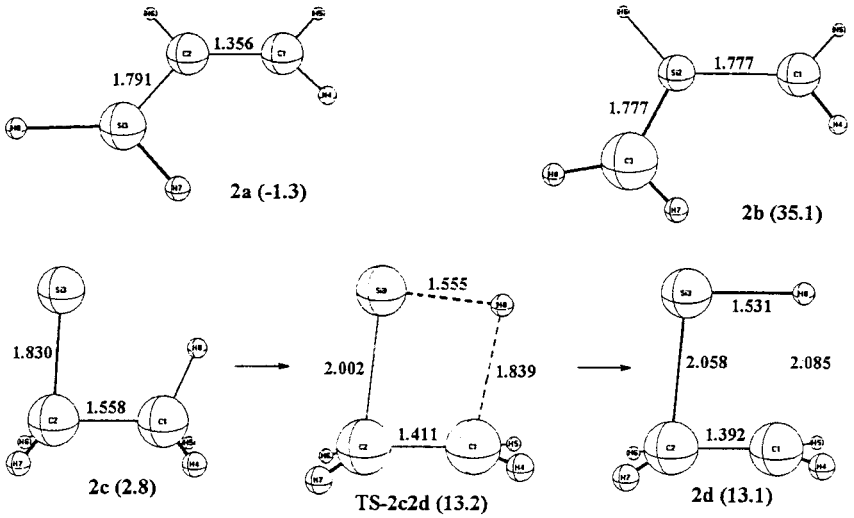

Figure 4. Structures of the $SiC_2H_5^+ + H$ system at the DFT(B3LYP)/6-311G(d,p) level of theory. Distances are in angstroms. Differences in free energy in kcal mol^{-1} with respect to isolated reactants $SiH_2^+ + C_2H_4$ are given in parentheses.

TABLE 4: Enthalpies and Free Energies (kcal mol^{-1}) at 298 K of the $SiC_2H_5^+ + H$ System Relative to Reactants $SiH_2^+ + C_2H_4$ at Various Levels of Theory

	DFT(B3LYP)/ 6-311G(d,p)		CBS-Q		G2	
species	ΔH_{298}	ΔG_{298}	ΔH_{298}	ΔG_{298}	ΔH_{298}	ΔG_{298}
2a + H	−4.7	−1.3	−8.2	−4.8	−8.5	−5.2
2b + H	32.1	35.1	25.5	28.4	24.4	27.2
2c + H	−0.7	2.8	−5.8	−2.4	−6.0	−2.5
2d + H	9.5	13.1	6.2	9.4	6.0	9.1
TS-2c2d + H	8.9	13.2				

TABLE 5: Enthalpies and Free Energies (kcal mol^{-1}) at 298 K of the $SiC_2H_4^{\bullet+} + H_2$ System Relative to Reactants $SiH_2^+ + C_2H_4$ at Various Levels of Theory

	DFT(B3LYP)/ 6-311G(d,p)			CBS-Q		G2	
species	ΔH_{298}	ΔG_{298}	$\langle S^2\rangle$	ΔH_{298}	ΔG_{298}	ΔH_{298}	ΔG_{298}
3a + H_2	−25.4	−23.2	0.7528	−27.7	−25.7	−26.9	−25.0
3b + H_2	−19.8	−17.6	0.7530	−21.6	−19.3	−20.3	−18.1
3c + H_2	−22.7	−20.8	0.7530	−22.3	−20.6	−21.7	−19.9
3d + H_2	−7.6	−5.8	0.7522	−13.1	−10.6	−12.0	−9.6
TS-1a3a + H_2	14.7	25.6	0.7546				
TS-1a3b + H_2	−6.8	4.2	0.7714				
TS-1b3b + H_2	18.5	29.3	0.7581				
TS-1b3c + H_2	−8.0	3.0	0.7669				
TS-3a3b + H_2	9.6	11.7	0.7620				
TS-3a3c + H_2	2.4	4.9	0.7589				
TS-3b3c + H_2	3.3	6.2	0.7685				
TS-3b3d + H_2	6.0	8.7	0.7589				

may in principle be bonded both to the silicon atom or one to silicon and the other to either carbon atom. However, not all the transition structures for H_2 elimination are attainable at thermal energies. Whereas TS-**1a3b** and TS-**1b3c** correspond to barriers barely in excess of the reactants energy, TS-**1a3a** and TS-**1b3b** lie well above the energy of reactants and are relevant to hardly viable pathways. In the hypothesis that thermal energy from collisions is available, the most favorable paths appear to be

$$\mathbf{1a} \rightarrow \text{TS-}\mathbf{1a3b} \rightarrow \mathbf{3b} \qquad (13)$$

$$\mathbf{1a} \rightarrow \text{TS-}\mathbf{1a1b} \rightarrow \mathbf{1b} \rightarrow \text{TS-}\mathbf{1b3c} \rightarrow \mathbf{3c} \qquad (14)$$

Whether the two lower barriers can be surmounted at thermal energies depends both on the accuracy of their computational estimate and on the detailed dynamics of the system. All the $SiC_2H_4^{\bullet+} + H_2$ minima have lower free energy than the $SiC_2H_5^+ + H$ system. As was the case with the $SiC_2H_6^{\bullet+}$ ions, there are transition structures for 1,2 (TS-**3a3b,** TS-**3a3c**) and 1,3 hydrogen migrations (TS-**3b3d**, TS-**3b3c**) connecting the intermediates. These have barriers above the average thermal energies of the isolated reactants and thus are not attainable by the system whenever it is far from thermal equilibrium (Figure 5).

The bridged structure **3a** is the most stable species. Its silicon atom interacts symmetrically with the two carbon atoms of ethene and the C−C distance is elongated by 0.070 Å with respect to ethene. Structure **3d** is also bridged with its silicon atom interacting with the π system of the ethyne-like moiety, whose C−C distance is elongated 0.059 Å. The spin densities are equally shared between the two interacting fragments in **3a** and **3d**, while in isomers **3b** and **3c**, the unpaired electron is mainly localized on the SiH and CH groups, respectively.

D. CH_3 Dissociation from $SiC_2H_6^{\bullet+}$ to $SiCH_3^+$ Ions. Structure **4a** (Figure 6, Table 6) originates from a homolytic cleavage of the Si−C bond in compound **1d**. The endothermic process from **1a** to **4a** involves crossing structures TS-**1a1b**, **1b**, TS-**1b1c**, **1c**, and TS-**1c1d** as reported in Figure 3. Only TS-**1c1d** has energy in excess of reactants. A structure $H_2C{=}SiH^+$ (**4b**) has been located ($\Delta G = 23.0$ kcal mol^{-1}); its formation goes through homolytic cleavage of the C−C bond in **1b**. Structure **4b** has not been confirmed by the MP2/6-31G(d) optimization prior to the CBS-Q and G2 methods.

E. Thermochemistry. The enthalpies of formation at 298 *K* of compounds **1a**−**1e**, **2a**−**2d**, **3a**−**3d**, and **4a** have been computed at the DFT(B3LYP)/6-311G(d,p)//DFT(B3LYP)/6-311G(d,p), CBS-Q, and G2 level of theory. The ΔH°_{298} values calculated in this study are shown in Table 7 together with both experimental and computed values reported in the literature. These enthalpies correspond to the processes:

$$Si^+_{(g)} + 2C_{(s)} + 3H_{2(g)} \rightarrow SiC_2H_6^{\bullet+} \qquad (15)$$

$$Si^+_{(g)} + 2C_{(s)} + {}^5/_2H_{2(g)} \rightarrow SiC_2H_5^+ \qquad (16)$$

$$Si^+_{(g)} + 2C_{(s)} + 2H_{2(g)} \rightarrow SiC_2H_4^{\bullet+} \qquad (17)$$

$$Si^+_{(g)} + C_{(s)} + {}^3/_2H_{2(g)} \rightarrow SiCH_3^+ \qquad (18)$$

We made use of the experimental enthalpies of formation[40] of

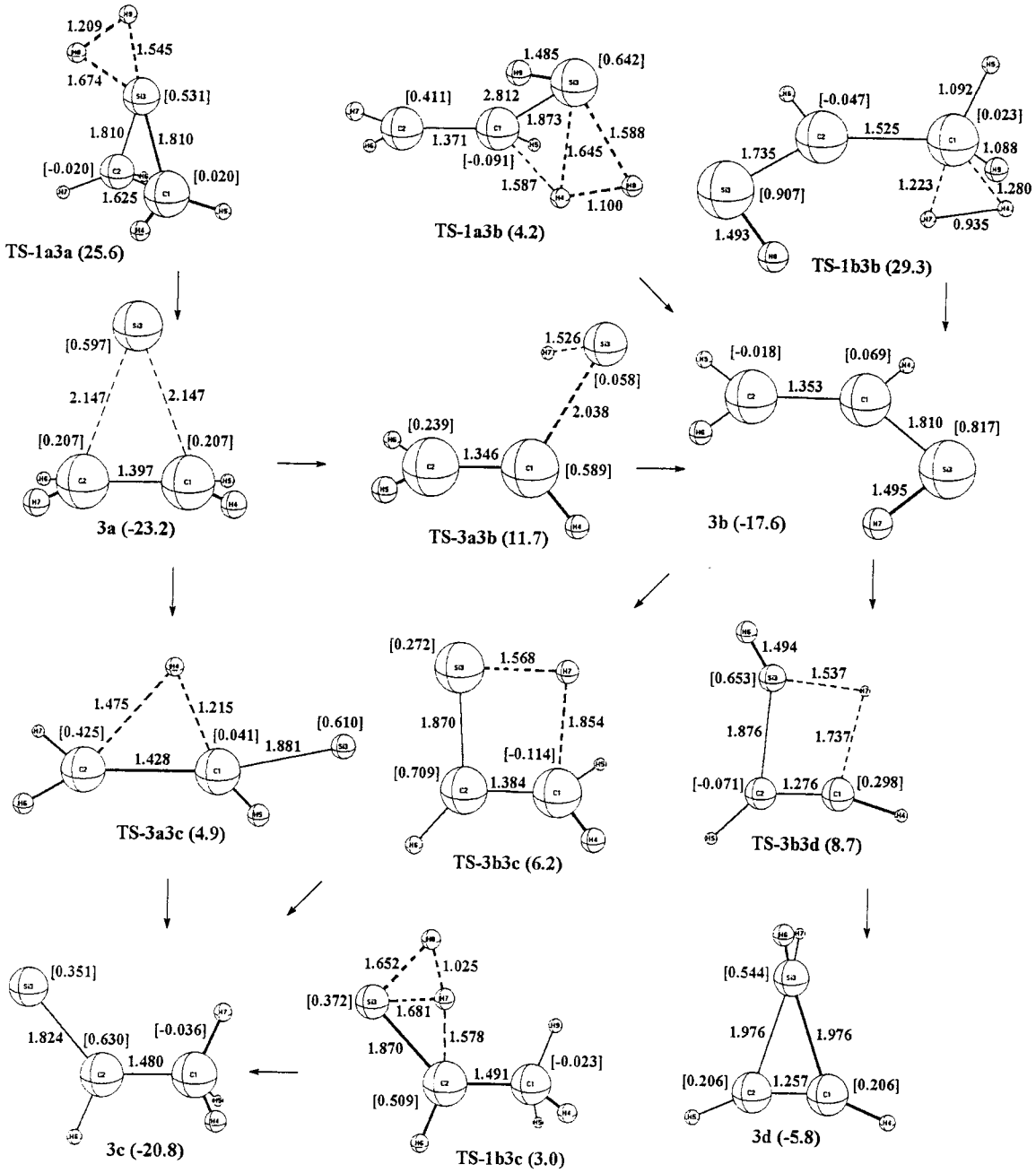

Figure 5. Intermediates and transition structures of the $SiC_2H_4^{\bullet+} + H_2$ system at the DFT(B3LYP)/6-311G(d,p) level of theory. Distances are in angstroms. Differences in free energy in kcal mol^{-1} with respect to isolated reactants $SiH_2^+ + C_2H_4$ are given in parentheses; total spin densities are given in brackets.

TABLE 6: Enthalpies and Free Energies (kcal mol^{-1}) at 298 K of the $SiCH_3^+ + CH_3$ System Relative to Reactants $SiH_2^+ + C_2H_4$ at Various Levels of Theory

	DFT(B3LYP)/6-311G(d,p)		CBS-Q		G2	
species	ΔH_{298}	ΔG_{298}	ΔH_{298}	ΔG_{298}	ΔH_{298}	ΔG_{298}
4a + CH_3	−15.7	−16.6	−16.7	−18.0	−16.8	−18.0
4b + CH_3	24.2	23.0				

gaseous carbon and silicon cation:

$$C_{(s)} \rightarrow C_{(g)}\,(^3P) \quad (\Delta H^\circ = 171.3 \text{ kcal mol}^{-1}) \qquad (19)$$

$$Si_{(s)} \rightarrow Si^+_{(g)}\,(^2P) + e \quad (\Delta H^\circ = 295 \text{ kcal mol}^{-1}) \qquad (20)$$

The data from the three sets of calculations are in good agreement, their standard deviations ranging from 0.19 kcal mol^{-1} for compound **1b** to 4.1 kcal mol^{-1} for compound **2b**. Among species **1**, **2**, **3**, and **4**, we can identify a most stable species whose computed enthalpy of formation is close to the experimental value, suggesting its structure as the more favor-

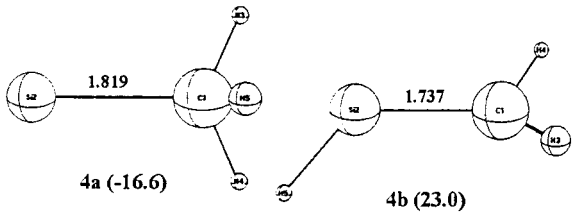

Figure 6. Structures of the $SiCH_3^+ + CH_3$ system at the DFT(B3LYP)/6-311G(d,p) level of theory. Distances are in angstroms. Differences in free energy in kcal mol^{-1} with respect to isolated reactants $SiH_2^+ + C_2H_4$ are given in parentheses.

TABLE 7: Computed Enthalpies of Formation at 298 K (ΔH°_{298})[a] of the $SiC_2H_6^{\bullet+}$, $SiC_2H_5^+$, $SiC_2H_4^{\bullet+}$, and $SiCH_3^+$ Species at the DFT(B3LYP)/6-311G(d,p), CBS-Q, and G2 Level of Theory

species	DFT(B3LYP) 6-311G(d,p)	CBS-Q	G2	μ[b]	σ[b]	previous data
$SiC_2H_6^{\bullet+}$						217.1,[c] 210.2,[c] <275[d]
$2C + Si^+ + 3H_2$	0.0	0.0	0.0			
1a	236.2	233.0	233.1	234.1	1.8	
1b	243.4	243.1	243.0	243.2	0.19	
1c	254.4	253.2	252.5	253.4	0.96	
1d	222.3	221.2	223.6	222.4	1.2	
1e	237.4	238.6	241.1	239.0	1.9	
SiC_2H_5+						230.3[e]
$2C + Si^+ + 5/2H_2$	0.0	0.0	0.0			
2a	233.7	230.7	229.8	231.4	2.0	
2b	270.5	264.4	262.7	265.9	4.1	
2c	237.7	233.0	232.3	234.3	2.9	
2d	247.9	245.1	244.3	245.8	1.9	
$SiC_2H_4^{\bullet+}$						<275,[d] <277,[e] 260.3[f]
$2C + Si^+ + 2H_2$	0.0	0.0	0.0			
3a	265.3	263.9	264.0	264.4	0.78	
3b	270.9	270.0	270.6	270.5	0.46	
3c	268.0	269.2	269.2	268.8	0.69	
3d	283.1	278.5	278.9	280.2	2.5	
$SiCH_3^+$						230,[d] <242.3,[e] 233.9,[f] 235.8,[f] <289,[g] 231,[h] 235[h]
$C + Si^+ + 3/2H_2$	0.0	0.0	0.0			
4a	240.0	237.8	237.3	238.4	1.4	
4b	279.9					

[a] In kcal mol^{-1}. [b] Mean values (μ) and standard deviations (σ) between the three computational methods. [c] Reference 43. [d] Reference 22. [e] Reference 23. [f] Reference 26. [g] Reference 44. [h] Reference 45.

able. In particular, compounds **1d**, **2a**, **3a**, and **4a** with enthalpies of formation of 222.4, 231.4, 264.4, and 238.4 kcal mol^{-1}, respectively, can be identified with the actual species formed in the first step of the processes described in Scheme 2.

Conclusions

The investigation of the gas-phase ion/molecule processes in silane/ethene systems has provided valuable information on (i) experimental conditions, reaction mechanisms, and kinetics which favor the formation of silicon- and carbon-containing ion species of increasing size; (ii) structures, energy profiles, and thermodynamical data of intermediates and products originated from C_2H_4 and SiH_2^+, which is the most reactive among primary ions of silane.

The formation and growth of mixed ion aggregates is favored in mixtures containing an excess of silane, their yield being high even at short reaction times. As a consequence, in a flow system, it is possible to modulate the relative amount of the reactants in order to prepare species containing Si−C bonds, leading eventually to amorphous silicon carbides of desired composition. The chain propagation mainly starts from ions of silane reacting with ethene molecules. Systems with similar partial pressures of SiH_4 and C_2H_4 yield mixed condensates in amounts which are only slightly lower than those with silane in excess. This trend is likely due to the formation of SiH_n^+ ions also from $C_2H_n^+$ species reacting with silane.

Experimental results show that SiH_2^+ plays a major role in the formation of mixed ions. Therefore, its reactions with ethene have been investigated by high-level theoretical methods. Hydrogen atom, hydrogen molecule, and methyl dissociation from the initial adduct, as well as from isomer ions, have been considered. The free energy release in the $SiC_2H_6^{\bullet+}$ adduct formation **1a**, is estimated to be 44 kcal mol^{-1} and sets a reference value for determining which processes are attainable. It has been assessed that four more isomers are attainable by passing through transition structures of energy lower or comparable with that of reactants. The H atom dissociation that gives $SiC_2H_5^+$ ion species presents three viable pathways from different $SiC_2H_6^{\bullet+}$ isomers to the **2a** and **2c** structures, involving homolytic cleavage of a C−H or a Si−H bond. The dissociation process of a hydrogen molecule from $SiC_2H_6^{\bullet+}$ ions could give four $SiC_2H_4^{\bullet+}$ isomers. However, only two of them, **3b** and **3c**, are formed directly through accessible paths from **1a** and **1b**, respectively, as the corresponding transition states show barriers barely in excess of the reactant energy. Moreover, isomerization of **3c** to **3a**, the most stable structure among $SiC_2H_4^{\bullet+}$ ions, represents also a viable reaction. The dissociation of the methyl group occurs through a complex process which consists of three successive isomerization steps to **1d** (the last transition structure being slightly higher than the mentioned reference energy value) followed by homolytic cleavage of a Si−C bond.

The energy differences of the pathways determined by theoretical calculations are rather small, and this suggests that the system proceeds toward different products without specific preferences. On the other hand, the description provided by theoretical methods is in good agreement with the experimental kinetic constants for reactions of SiH_2^+ with C_2H_4 (Table 1), whose ratios are never larger than 10. Finally, the theoretically computed enthalpies of formation of the most stable $SiC_2H_6^{\bullet+}$, $SiC_2H_5^+$, $SiC_2H_4^{\bullet+}$, and $SiCH_3^+$ structures show fairly good agreement with the data reported in the literature.

Acknowledgment. The authors acknowledge the Italian Ministero dell'Università e della Ricerca Scientifica e Tecnologica and the University of Torino for financial support.

References and Notes

(1) Petrie, S.; Bohme, D. K. *Astrophys. J.* **1994**, *436*, 411.
(2) Petrie, S.; Becker, H.; Baranov, V.; Bohme, D. K. *Astrophys. J.* **1997**, *476*, 191.
(3) Reents, W. D., Jr.; Mandich, M. L. *J. Chem. Phys.* **1992**, *96*, 4429 and references therein.
(4) Operti, L.; Splendore, M.; Vaglio, G. A.; Franklin, A. M.; Todd, J. F. J. *Int. J. Mass Spectrom. Ion Processes* **1994**, *136*, 25.
(5) Stinespring, C. D.; Wormhoudt, J. C. *J. Cryst. Growth* **1988**, *87*, 481.

(6) Allendorf, M. D.; Kee, R. J. *J. Electrochem. Soc.* **1991**, *138*, 841.
(7) Speranza, M. *Trends Organomet. Chem.* **1994**, *1*, 35.
(8) Schröder, D.; Heineman, C.; Koch, W.; Schwarz, H. *Pure Appl. Chem.* **1997**, *69*, 273.
(9) Cacace, F. *Pure Appl. Chem.* **1997**, *69*, 227.
(10) Benzi, P.; Operti, L.; Vaglio, G. A.; Volpe, P.; Speranza, M.; Gabrielli, R. *Int. J. Mass Spectrom. Ion Processes* **1990**, *100*, 647.
(11) Haller, I. *J. Phys. Chem.* **1990**, *94*, 4135.
(12) Cacace, F.; Speranza, M. *Science* **1994**, *265*, 208.
(13) Bowers, M. T.; Marshall, A. G.; McLafferty, F. W. *J. Phys. Chem.* **1996**, *100*, 12897.
(14) Cetini, G.; Operti, L.; Rabezzana, R.; Vaglio, G. A.; Volpe, P. *J. Organomet. Chem.* **1996**, *519*, 169.
(15) Antoniotti, P.; Operti, L.; Rabezzana, R.; Vaglio, G. A.; Volpe, P.; Gal, J. F.; Grover, R.; Maria, P. C. *J. Phys. Chem.* **1996**, *100*, 155.
(16) Raghavachari, K. *J. Chem. Phys.* **1992**, *96*, 4440 and references therein.
(17) (a) Antoniotti, P.; Operti, L.; Rabezzana, R.; Splendore, M.; Tonachini, G.; Vaglio, G. A. *J. Chem. Phys.* **1997**, *107*, 1491. (b) Antoniotti, P.; Operti, L.; Rabezzana, R.; Tonachini, G.; Vaglio, G. A. *J. Chem. Phys.* **1998**, *109*, 10853.
(18) Cruz, E. M.; Lopez, X.; Ayerbe, M.; Ugalde, J. M. *J. Phys. Chem.* **1997**, *101*, 2166.
(19) Gal, J. F.; Grover, R.; Maria, P. C.; Operti, L.; Rabezzana, R.; Vaglio, G. A.; Volpe, P. *J. Phys. Chem.* **1994**, *98*, 11978.
(20) Mayer, T. M.; Lampe, F. W. *J. Phys. Chem.* **1974**, *78*, 2433.
(21) Allen, W. N.; Lampe, F. W. *J. Am. Chem. Soc.* **1977**, *99*, 6816.
(22) Wlodek, S.; Fox, A.; Bohme, D. K. *J. Am. Chem. Soc.* **1991**, *113*, 4461.
(23) Boo, B. H.; Armentrout, P. B. *J. Am. Chem. Soc.* **1991**, *113*, 6401.
(24) Ketvirtis, A. E.; Bohme, D. K.; Hopkinson, A. C. *J. Mol. Struct. (THEOCHEM)* **1994**, *313*, 1.
(25) Antoniotti, P.; Operti, L.; Rabezzana, R.; Vaglio, G. A.; Volpe, P. *Int. J. Mass Spectrom.* **1999**, *190/191*, 243.
(26) Ketvirtis, A. E.; Bohme, D. K.; Hopkinson, A. C. *J. Phys. Chem.* **1995**, *99*, 16121.
(27) Moc, J.; Nguyen, K. A.; Gordon, M. S. *Orgnometallics* **1996**, *15*, 5391.
(28) Bottoni, A. *J. Phys. Chem. A* **1997**, *101*, 4402.
(29) Decouzon, M.; Gal, J. F.; Maria, P. C.; Tchinianga, A. S. Personal communication.
(30) Gonzales, C.; Schlegel, H. B. *J. Chem. Phys.* **1989**, *90*, 2154.
(31) Frisch, M. J.; Trucks, G. W.; Schlegel, H. B.; Gill, P. M. W.; Johnson, B. G.; Robb, M. A.; Cheeseman, J. R.; Keith, T. A.; Peterson, G. A.; Montgomery, J. A.; Raghavachari, K.; Al-laham, M. A.; Zakrzewski, V. G.; Ortiz, J. V.; Foresman, J. B.; Cioslowski, J.; Stefanov, B. B.; Nanayakkara, A.; Challacombe, M.; Peng, C. Y.; Ayala, P. Y.; Wong, M. W.; Replogle, E. S.; Gomperts, R.; Andres, J. L.; Martin, R. L.; Fox, D. J.; Binkley, J. S.; DeFrees, D. J.; Baker, J.; Stewart, J. J. P.; Head-Gordon, M.; Gonzales, C.; Pople, J. A. *GAUSSIAN94*; Gaussian Inc.: Pittsburgh, PA, 1995.
(32) (a) Becke, A. D. *J. Chem. Phys.* **1993**, *98*, 5648. (b) Lee, C.; Yang, W.; Parr, R. G. *Phys. Rev.* **1988**, *B37*, 785. (c) Miehlich, B.; Savin, A.; Stoll, H.; Preuss, H. *Chem. Phys. Lett.* **1989**, *157*, 200. (d) Hariharan; P. C.; Pople, J. A. *Theor. Chim. Acta* **1973**, *28*, 213. Frisch, M. J.; Pople, J. A.; Binkley, J. S. *J. Chem. Phys.* **1984**, *80*, 3265.
(33) Petersson, G. A.; Tensfeldt, T. G.; Montgomery, J. A., Jr. *J. Chem. Phys.* **1991**, *94*, 6091.
(34) Curtiss, L. A.; Raghavachari, K.; Trucks, G. W.; Pople, J. A. *J. Chem. Phys.* **1991**, *94*, 7221.
(35) Hehre, W. J.; Radom, L.; Schleyer, P.v. R.; Pople, J. A. In *Ab Initio Molecular Orbital Theory*; Wiley: New York, 1986.
(36) Wittbrodt, J. M.; Schlegel, H. B. *J. Chem. Phys.* **1996**, *105*, 6574.
(37) Kerr, J. A. In *Handbook of Physics and Chemistry*, 73rd ed.; CRC Press: London, 1992−93.
(38) Bowers, M. T. In *Gas-Phase Ion Chemistry*; Academic Press: New York, 1979; Vol. 1.
(39) Lippincot, E. R.; Stutman, J. A. *J. Phys. Chem.* **1964**, *68*, 296.
(40) Kirouac, S.; Bose, T. K. *J. Chem. Phys.* **1976**, *64*, 1580.
(41) See, for example: Kim, J. K.; Anicich, V. G.; Huntress, W. T., Jr. *J. Phys. Chem.* **1977**, *81*, 1798.
(42) Lias, S. G.; Bartmess, J. E.; Liebman, J. F.; Holmes, J. L.; Levin, R. D.; Mallard, W. G. *J. Phys. Chem. Ref. Data Suppl.* **1988**, *17*.
(43) Shin, S. K.; Corderman, R. R.; Beauchamp J. L. *Int. J. Mass Spectrom. Ion Processes* **1990**, *101*, 257.
(44) Stewart, G. W.; Herris, J. M. S.; Gaspar, P. P. *J. Chem. Phys.* **1972**, *57*, 1990.
(45) Boo, B. H.; Elkind, J. L.; Armentrout, P. B. *J. Am. Chem. Soc.* **1990**, *112*, 2083.